Astron. Astrophys. 219, 205–218 (1989)

ASTRONOMY AND ASTROPHYSICS

Radiation-driven winds of hot stars

VI. Analytical solutions for wind models including the finite cone angle effect

R.P. Kudritzki[1], A. Pauldrach[1], J. Puls[1], and D.C. Abbott[2]

[1] Institut für Astronomie und Astrophysik der Universität München, Scheinerstrasse 1, D-8000 München 80, Federal Republic of Germany
[2] Joint Institute for Laboratory Astrophysics, University of Colorado, Campus Box 440, Boulder, CO 80309, USA

Received November 4, accepted December 15, 1988

Summary. Analytical solutions for radiation-driven winds of hot stars including the important finite cone angle effect (see Pauldrach et al., 1986; Friend and Abbott, 1986) are derived which approximate the detailed numerical solutions of the exact wind equation of motion very well. They allow a detailed discussion of the finite cone angle effect and provide for given line force parameters k, α, δ definite formulae for mass-loss rate $\dot{M}$ and terminal velocity v_∞ as function of stellar parameters.

Key words: stellar winds – hot stars – mass loss

1. Introduction

The theory of radiation driven winds after its recent significant improvements appears to be a very promising tool to describe the observed winds and mass-loss of hot stars in a quantitative way. The original concept by Castor, Abbott and Klein (1975, "CAK") was further developed by Abbott (1982), who provided a realistic line list of 250000 lines contributing to the line force. Pauldrach, Puls and Kudritzki (1986, "PPK") and Friend and Abbott (1986, "FA") independently investigated the importance of the finite cone angle effect, which modifies the wind dynamics significantly and leads to a convincing general agreement with the observations (see also Kudritzki et al., 1987). Pauldrach (1987) dropped the approximative treatment of metal occupation numbers and treated for the first time the full NLTE multi level problem by solving the rate equations for 133 ions (including electron collisions and correct continuum radiative transfer) simultaneously with radiation driven wind hydrodynamics. In this way, he obtained a strong shift towards higher ionization stages, which at least partially solved the long-standing problem of "superionization" in cool winds without any extra source of ionization. Puls (1987) extended this work further by including additonally in a selfconsistent realistic way the important effect of overlapping lines, which was investigated in a somewhat more simplified manner before by Panagia and Machetto (1982) and Friend and Castor (1983). Thus, wind models for hot stars are now available, which treat the physics of the interaction between driving photospheric photons and wind plasma in a very detailed and realistic way. At the moment, these extensive models are being applied on a variety of cases: Massive stars in different evolutionary stages (Pauldrach et al., 1989) and with different metallicity, Central Stars of Planetary Nebulae (Pauldrach et al., 1988), hot subdwarfs, supermassive stars etc. The computational effort for these calculations is enormous, since, besides the detailed microphysics, complicated and sometimes slowly convergent iteration cycles are involved. It is therefore desirable to have practicable analytical solutions, which can be used as a first iteration step and which are already close to the final solution. Moreover, these analytical solutions can provide a deeper understanding of the complex computer code results. Finally, the analytical solutions yield also definite formulas for mass-loss rate $\dot{M}$ and terminal velocity v_∞ as function of the stellar parameters, which are the basic observational dynamical wind quantities. Such formulae are very useful for the comparison with the observational data and can also be used as input for stellar evolution codes, which have to include the effects of mass-loss along the tracks.

The old theory by CAK allows one to derive such formulae in a simple way (see also Abbott, 1978, 1980, 1982). For the improved models including the finite cone angle effect no analytical solutions have been provided yet. PPK have given complicated formulae for $\dot{M}$ and v_∞, which however require the knowledge of the radial coordinate of the critical point and fail if this value is not close to unity as in case of supergiants and Central Stars of Planetary Nebulae. FA obtained a simple formula for v_∞ as a result of a least square fit procedure to their numerical results. This formula however neglects the influence of δ, the second line force multiplier parameter, which was introduced by Abbott (1982) to describe the back reaction of the line force on changes of the ionization structure in the wind. As we shall show below, this is a non-negligible effect. In addition, the dependence of the ratio v_∞/v_{esc} on v_{esc} (the surface escape velocity) is not described completely by this formula. FA adopted v_∞/v_{esc} to depend on v_{esc} only, whereas we will show that it depends on the scale height of the photosphere in units of stellar radius, which is given by the ratio of v_s^2/v_{esc}^2 (v_s is the isothermal sound speed). Although this is of little importance for the practical fitting of massive O-star observations, it has some relevance in the case of Central Stars, where much hotter photospheric temperatures and lower escape velocities are encountered (see Méndez et al., 1985, 1988; Kudritzki and Méndez, 1988).

The motivation for the paper therefore is to develop analytical solutions for the velocity and density structure of radiation driven winds, which include the finite cone angle effect. These solutions

Send offprint requests to: R.P. Kudritzki

will provide analytical expressions for v_∞ and $\dot{M}$ for all realistic values of the force multiplier parameters α and δ ($0.5 \leq \alpha \leq 0.75$, $0.01 \leq \delta \leq 0.1$) and also for the case of extended photospheres, which are characterized by relatively large values of v_s^2/v_{esc}^2. These formulae can be used in all cases where good first estimates are needed, as for instance in the case of stellar evolution, observational spectroscopy, energy or momentum input onto the Interstellar Medium or Planetary Nebulae. The structure of the paper is as follows: In Sect. 2 the general concept is developed. Section 3 gives as a simple first example the application on the CAK case without finite cone angle correction. This correction is then taken into account in Sect. 4 for thin ($v_s^2/v_{esc}^2 \ll 1$) and in Sect. 5 for extended ($v_s^2/v_{esc}^2 < 1$) photospheres. Section 6 gives the final cooking recipe to compute $\dot{M}$ and v_∞. Section 7 finally compares with detailed numerical calculations.

2. The theory of radiation-driven winds and our basic concept for analytical solutions

In its present status the theory of radiation driven winds treats stationary radial symmetric one component flows ignoring viscosity, heat conduction and (with some exceptions, see PPK, FA and Friend and Mc Gregor, 1984) magnetic fields and rotation. The equation of motion is then given by

$$v\frac{dv}{dr} = -\frac{1}{\rho(r)}\frac{dp}{dr} - \frac{GM_*}{r^2} + g_{\text{rad}}^{\text{Th}}\left(1 + M\left(\rho, v, \frac{dv}{dr}, r, n_E\right)\right). \quad (1)$$

All quantities have the usual meaning (see for instance PPK). $g_{\text{rad}}^{\text{Th}}$ is the radiative acceleration caused by Thomson scattering and $M(\rho, v, dv/dr, n_E)$ is the "force multiplier" – the line force in units of the Thomson-scattering force. This is the crucial quantity in radiation driven winds. As shown originally by Abbott (1982), and later by PPK, Kudritzki et al. (1987), Pauldrach (1987), Puls (1987) a very useful parametrization of the force multiplier is given by

$$M\left(\rho, v, \frac{dv}{dr}, r, n_E\right) = k\left(\frac{\sigma_E \rho v_{th}}{dv/dr}\right)^{-\alpha}\left(\frac{n_E}{W(r)}\right)^{\delta} CF\left(r, v, \frac{dv}{dr}\right) \quad (2)$$

v_{th} is the thermal velocity of the protons. $\sigma_E\rho$ is the Thomson scattering absorption coefficient, $n_E(r)$ the electron density (in 10^{11} cm^{-3}) and

$$W(r) = 0.5(1-(1-(R_*/r)^2)^{1/2} \quad (3)$$

the dilution factor. The parameters k, α, δ are obtained from the detailed NLTE calculations for all the individual lines contributing to the line force. Roughly speaking k represents the number of lines with strengths larger than a critical value, α the slope of the line strength distribution function and δ the change in ionization due to changes in the ionization and recombination rate. We have to note here that in recent work by Pauldrach (1987) the parameter triple (k, α, δ) is not held fixed anymore in the entire wind, but is allowed to vary instead. However, it is always possible to define depth independent mean values, which represent the final solution very well (see for instance Puls, 1987). Thus, we regard in the following k, α, δ as depth independent. The finite cone angle correction factor CF (see PPK, FA or also CAK) is given by

$$CF = \frac{1}{\alpha+1}\frac{x^2}{1-h}\left(1-\left(1-\frac{1}{x^2}+\frac{h}{x^2}\right)^{\alpha+1}\right)$$

$$\frac{1}{h} = \frac{d\ln v}{d\ln x}, \quad (4)$$

where $x = r/R_*$ is the dimensionless radial coordinate.

We now restrict ourselves to the case of an isothermal wind, which is a good approximation for cool radiation driven winds (see PPK). Then we have $p = v_s^2\rho$ with $v_s = \text{const}$, which together with $\dot{M} = 4\pi r^2 \rho v$ – the equation of mass conservation – yields the well known non-linear implicit differential equation for the velocity field of radiation driven winds (see CAK, PPK, FA):

$$F(x, y, v) = C f(x, y, v) y^\alpha - A\left(1-\frac{4v_s^2}{v_{esc}^2}x\right) - y\left(1-\frac{v_s^2}{v^2}\right) \equiv 0. \quad (5)$$

Here the following abbreviations are used: y is related to the velocity gradient and defined as

$$y = r^2 v\frac{dv}{dr} = R_* x^2 v\frac{dv}{dx}. \quad (6)$$

v_{esc} is the photospheric escape velocity reduced by the accelerating contribution of Thomson scattering

$$v_{esc} = (2g(1-\Gamma)R_*)^{1/2}, \quad (7)$$

where Γ is given by $\Gamma = L/L_E$ the ratio of stellar to Eddington luminosity. The constant A is related to v_{esc} by

$$A = v_{esc}^2 R_*/2. \quad (8)$$

The function f is the product of finite cone angle correction factor CF and the δ-dependent ionization correction

$$f(x, y, v, \alpha, \delta) = \left(\frac{n_E}{W}\right)^{\delta} CF(x, y, v, \alpha). \quad (9)$$

It is assumed that $n_E \sim \rho \sim (x^2 v)^{-1}$ in this definition of f. The constant C is given by

$$C = \frac{L\sigma_E}{4\pi c} k\left(\frac{4\pi}{\sigma_E v_{th}\dot{M}}\right)^{\alpha}. \quad (10)$$

Besides the numerical solution of Eq. (5), the determination of C – the eigenvalue of the problem – is crucial. It is usually determined from the singularity of Eq. (5) at its critical point x_c, which is found by the singularity condition

$$\left.\frac{\delta F}{\delta y}\right|_{x=x_c} = 0 \quad (11)$$

and by the regularity condition

$$\left.\left(\frac{\delta F}{\delta x} + \frac{\delta F}{\delta v}\frac{\delta v}{\delta x}\right)\right|_{x=x_c} = 0. \quad (12)$$

Equations (5), (11) and (12) together with the constraint on the optical depth integral

$$\int_{R_*}^{\infty} \rho(r)\sigma_E\, dr = 2/3$$

yield x_c, v_c, y_c and C at the critical point. Then, $v(x)$ is obtained by integrating numerically away from the critical point (inward and outward) along the appropriate solution branches of Eq. (5).

Our approximate analytical treatment is different. It uses an approximation for the function $f(x, y, v, \alpha, \delta)$, which follows from the results obtained by PPK, who have found that the assumption $h \ll 1$ (i.e. $(v/r)/(dv/dr) \ll 1$) is a good first iteration step for the function CF. Moreover, PPK have found that

$$v(x) \approx v_\infty \left(1 - \frac{1}{x}\right)^\beta, \quad \text{for } x > x_c \tag{13}$$

is an excellent approximation for the correct numerical solution of the problem. Typical values for β are between 0.7 and 1.0. According to Eq. (4) we obtain for h in this case

$$h(x, \beta) = \frac{x-1}{\beta}. \tag{14}$$

In this approximation CF becomes a function of x, α, β only:

$$CF(x, \alpha, \beta) = \frac{1}{\alpha+1} \frac{x^2}{1-h(x,\beta)} \left(1 - \left(1 - \frac{1}{x^2} + h(x,\beta)\frac{1}{x^2}\right)^{\alpha+1}\right). \tag{15}$$

Figure 1 shows the behaviour of CF for different values of α and β. (Note that $h \to 0$ corresponds formally to $\beta \to \infty$).

We see that differences of β between 0.5 and 1.0 do not have extreme influence on CF. Even the case $\beta = \infty$ ($h = 0$) is not too far from the other curves, in particular if x is close to unity. Thus, we conclude that $CF(x, \alpha, \beta)$ as in Eq. (15) with $\beta \approx 1.0$ is a reasonable approximation for CF.

We now assume for a moment that δ is equal to zero. Then we have according to Eq. (9)

$$f(x, y, v, \alpha, \delta) = CF(x, \alpha, \beta) = f(x, \alpha, \beta) \tag{16}$$

which means that f is a function of x only. From Fig. 1 and Eq. (15) we realize that $f(x, \alpha, \beta)$ is monotonically increasing from $1 \le x \le 2(\beta+1)$ (a discussion of the functional behaviour of CF is given in the Appendix). This has important consequences for the solution of Eq. (5). At a given depth $x > x_c$ (where $v^2 \gg v_s^2$, see PPK) Eq. (5) reduces to a simple transcendental algebraic equation for y. The solution y_0 of this equation can be illustrated graphically as the intersection of $Cf(x, \alpha, \beta) y^\alpha$ with the linear curve $A(1 - 4xv_s^2/v_{esc}^2) + y$, as demonstrated in Fig. 2. (Note that

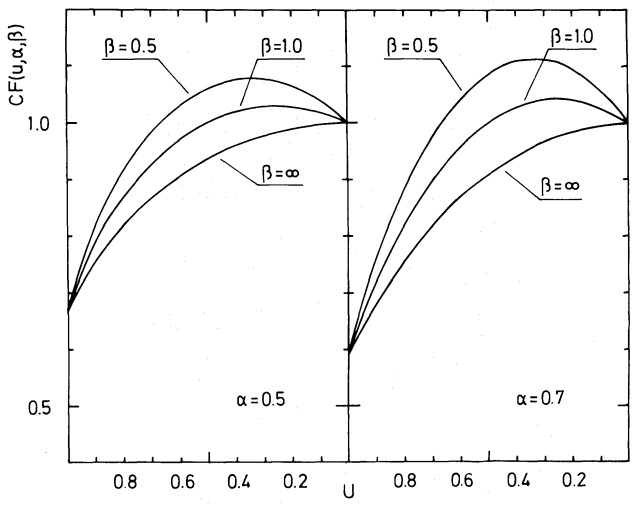

Fig. 1. The finite cone angle correction factor CF as function of reciprocal radius $u = 1/x$ for different values of α and β

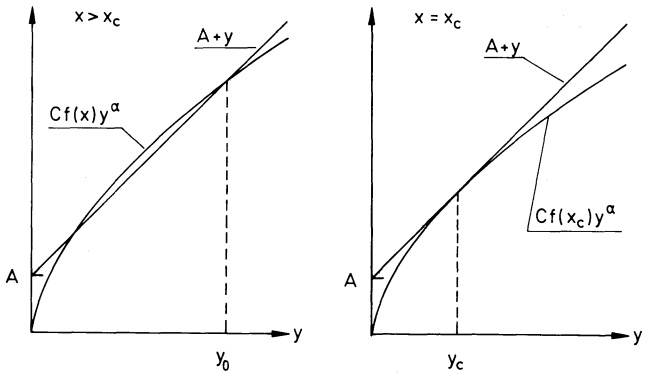

Fig. 2. The algebraic solution y_0 of Eq. (5) as the intersection of $Cf(x)y^\alpha$ and $A + y$ for a given $x > x_c$ and for $x = x_c$

the larger of the two intersection values is the appropriate one for $x > x_c$. Note also that normally $4v_s^2 x/v_{esc}^2 \ll 1$ for the region of significant wind acceleration.) If one approaches x_c from $x > x_c$, then $f(x, \alpha, \beta)$ becomes smaller because of its monotonic behaviour in x. Thus, there must exist a point where $A + y$ does not intersect but becomes tangent to Cfy^α (see Fig. 2b). This is just the critical point, since according to Eq. (11) it is defined by

$$\frac{d}{dy} Cf(x, \alpha, \delta) y^\alpha = \frac{d}{dy}(A(1 - v_s^2/v_{esc}^2 x) + y(1 - v_s^2/v^2)) \approx 1 \tag{17}$$

which is just the condition that at $x = x_c$ the slope of Cfy^α is equal to the slope of the linear curve $A + y$. (Note that this monotonic behaviour of f will not change if δ is nonzero. We will show that $(n_E/W)^\delta$ is only very slowly decreasing with increasing x).

Figure 2 contains the basic concept of our simplified analytical approach: In the following sections we will show that the intersection $y_0(x)$ at every depth $x \ge x_c$ can be approximated as an explicitly known function of x. This means that we can replace the implicit non-linear differential equation (5) by the simple explicite equation

$$\frac{dv^2}{dx} = \frac{2}{R_*} \frac{1}{x^2} y_0(x), \tag{18}$$

which is obtained from the definition of y, namely Eq. (6). The velocity field is then given by the integral

$$v^2(x) = v_c^2 + \frac{2}{R_*} \int_{x_c}^{x} \frac{1}{x^2} y_0(x)\, dx \tag{19a}$$

or with the substitution

$$u = \frac{1}{x}$$

$$v^2(u) = v_c^2 + \frac{2}{R_*} \int_{u}^{u_c} y_0(u)\, du. \tag{19b}$$

In a first step we will demonstrate the principles of this method for the simple case, when the approximations by CAK are used.

3. The simplest case: neglect of finite cone angle effects

The case $f(x, \alpha, \beta, \delta) \equiv 1$ corresponds to the radial streaming approximation by CAK, which neglects for the interaction between accelerating photons and wind plasma the photospheric finite cone angle, out of which the photons are streaming.

In a first step we discuss the critical point. From the singularity condition (Eq. 11) follows

$$C\alpha y_c^{\alpha-1}=1-\frac{v_s^2}{v_c^2}.$$

The combination of this expression with Eq. (5) yields the eigenvalue C

$$C=\frac{1-v_s^2/v_c^2}{\alpha}\,y_c^{1-\alpha} \tag{20}$$

and the velocity gradient y_c

$$y_c=\frac{\alpha}{1-\alpha}\,A\,\frac{1-4\,v_s^2\,x_c/v_{esc}^2}{1-v_s^2/v_c^2}. \tag{21}$$

The regularity condition (Eq. 12) yields

$$4x_c^2=\frac{v_{esc}^4}{v_c^4}\left(\frac{1-4v_s^2\,x/v_{esc}^2}{1-v_s^2/v_c^2}\right)^2\left(\frac{\alpha}{1-\alpha}\right)^2. \tag{22}$$

Now we take into account that according to CAK the coordinate x_s of the sonic point is close to unity (see also PPK). That means $v_s^2/v^2\ll 1$ for $x>1$. Moreover, we realize that normally $4v_s^2x/v_{esc}^2\ll 1$ for the accelerating part of the wind. From Eqs. (5) and (21) we then conclude

$$y_0(x)=y_c=\frac{\alpha}{1-\alpha}\,A \quad \text{for} \quad x>x_s. \tag{23}$$

That means that the intersection y_0 of Fig. 2 must be constant at all x, because $f(x,\alpha,\beta)$ is constant. With the definition of A (Eq. 8) the integral of Eq. (19) then yields

$$v^2(x)=\frac{\alpha}{1-\alpha}\,v_{esc}^2\left(\frac{1}{x_s}-\frac{1}{x}\right)+v_s^2, \tag{24}$$

which is the well known solution of CAK for $x>x_s$, which leads to

$$v_\infty^2=\frac{\alpha}{1-\alpha}\,v_{esc}^2. \tag{25}$$

Within these approximations we can also obtain the radius x_c of the critical point and the mass-loss rate $\dot{M}$. From Eq. (24) we have

$$v_c^2\approx\frac{\alpha}{1-\alpha}\,v_{esc}^2\left(1-\frac{1}{x_c}\right),$$

which yields together with Eq. (22)

$$x_c=1.5. \tag{26}$$

Equations (10), (19), (20) and (23) yield

$$\dot{M}_{CAK}=\left(\frac{\sigma_E}{4\pi c}\right)^{1/\alpha}\frac{4\pi}{\sigma_E v_{th}}\alpha k^{1/\alpha}\left(\frac{1-\alpha}{GM_*(1-\Gamma)}\right)^{(1-\alpha)/\alpha}L^{1/\alpha}. \tag{27}$$

This expression for the mass-loss rate is identical with CAK, although the way was derived is different. The same holds for Eq. (25), which describes the dependence of the terminal velocity on the photospheric surface velocity. The value for the critical point (Eq. 26) reproduces well the results of the detailed numerical calculations (see, for instance, PPK).

4. Finite cone angle effects: the case of geometrically very thin photopheres

Now we allow the function $f(x,\alpha,\beta,\delta)$ to vary as described by Eq. (9) and (15). This has two important effects: First $y_0(x)$ increases as function of x, as sketched in Fig. 2. This means that the radiative line acceleration of the flow increases strongly due to the fact that the radiation field becomes more and more radially peaked, when going outward. It is clear that this must change the wind dynamics significantly relative to the CAK case. The second effect is also caused by the variation of f and y_0 as function of x and concerns the radial coordinate x_c of the critical point. In the CAK case the real value of x_c is not important for $\dot{M}$ and $v(x)$, since f and therefore y_0 do not depend on x. In the finite cone angle case, however, the value of x_c is crucial, since the values of f at x_c determines the dynamics. We will show in the next section that the value of x_c is an monotonically increasing function of v_s^2/v_{esc}^2. (Note that $v_s^2/v_{esc}^2=\Delta r/R_*$, where Δr is the photospheric pressure scale height.) Thus, x_c is an increasing function of the geometrical photospheric extension, which is a very reasonable result. For $v_s^2/v_{esc}^2<3\,10^{-3}$, x_c comes close to unity (see next section or the numerical results by PPK). We will discuss this simpler case first and adopt for the rest of this section that $x_c\approx 1$.

4.1. *Frozen in ionization: the case $\delta=0$*

This case has been studied numerically by FA. Although it is somewhat unrealistic, it is the easier first step to include the finite cone angle effect. The function f is then given by Eq. (16) or (15) and Eq. (17) applied at $x_c\approx 1$ yields

$$C\,f(1,\alpha,\beta)\,\alpha y_0^{\alpha-1}(1)=1. \tag{28}$$

Again we have adopted that $v_s^2/v_c^2\ll 1$. On the other hand, we have from the equation of motion (Eq. 5)

$$C\,f(1,\alpha,\beta)\,y_0^\alpha(1)=A+y_0(1) \tag{29}$$

(see also Fig. 2). The combination of both equations yields

$$y_0(1)=\frac{\alpha}{1-\alpha}\,A$$

$$C=\frac{1}{f(1,\alpha,\beta)}\,\frac{1}{\alpha}\left(\frac{\alpha}{1-\alpha}\right)^{1-\alpha}A^{1-\alpha}. \tag{30}$$

Note that y_0 at the critical point is the same as in the CAK case. However, x_c is now close to unity contrary to 1.5 in the CAK case. Together with Eq. (10) this gives already the mass-loss rate

$$\dot{M}=f(1,\alpha,\beta)^{1/\alpha}\,\dot{M}_{CAK}, \tag{31}$$

where $\dot{M}_{CAK}$ is given by Eq. (27). Note that

$$f(1,\alpha,\beta)=\frac{1}{\alpha+1}. \tag{32}$$

Therefore, the mass-loss rate is smaller than in the simplified CAK-case, which just simply reflects that due to the finite cone angle of the photospheric disk the accelerating line force is smaller in the region around the critical point.

To calculate the velocity field according to Eq. (19) we need an estimate for $y_0(x)$ at $x>x_c\approx 1$ from the equation of motion (Eq. 5). For this purpose we determine first the value y_p, where the slope of $Cf(x,\alpha,\beta)y^\alpha$ is equal to unity, i.e. where Cfy^α turns over to intersect $y+A$ at y_0 (see Fig. 2). Because of $d/dy(Cfy^\alpha)=Cf\alpha y_p^{\alpha-1}=1$, we have

$$y_p=(Cf(x,\alpha,\beta)\,\alpha)^{1/1-\alpha}=\left(\frac{f(x,\alpha,\beta)}{f(1,\alpha,\beta)}\right)^{1/1-\alpha}\frac{\alpha}{1-\alpha}\,A. \tag{33}$$

Now we expand Cfy^α to second order around y_p to determine the intersection $y_0(x)$:

$$Cf(x,\alpha,\beta)y^\alpha = Cf(x,\alpha,\beta)y_p^\alpha + y - y_p + \frac{1}{y_p}(\alpha-1)\frac{1}{2}(y-y_p)^2.$$

(In this expansion $Cf\alpha y_p^{\alpha-1}=1$ was taken into account).

At the intersection of Cfy^α with $y+A$, which defines $y_0(x)$ we have

$$y_0 + A = Cfy_p^\alpha + y_0 - y_p + \frac{1}{y_p}(\alpha-1)\frac{1}{2}(y_0-y_p)^2,$$

which yields

$$y_0(x) = y_p + \left(\frac{2y_p}{1-\alpha}(Cfy_p^\alpha - A - y_p)\right)^{1/2}.$$

Inserting Eq. (33) and (30) we obtain after some calculation

$$y_0(x) = \frac{\alpha}{1-\alpha} A f_N(x,\alpha,\beta)^{1/1-\alpha} \times\left(1+\left(\frac{2}{\alpha}\left(1-\left(\frac{1}{f_N(x,\alpha,\beta)}\right)^{1/1-\alpha}\right)\right)^{1/2}\right). \quad (34)$$

The function f_N is the finite cone angle function now normalized at $x_c=1$.

$$f_N(x,\alpha,\beta) = f(x,\alpha,\beta)/f(1,\alpha,\beta). \quad (35)$$

Equation (34) for $y_0(x)$ (together with Eq. 8) now allows one to formulate the integral for the velocity according to Eq. (19)

$$v^2(u) = v_c^2 + \frac{\alpha}{1-\alpha} v_{esc}^2 \int_u^1 Z(u,\alpha,\beta)\,du$$

$$Z(u,\alpha,\beta) = f_N(u,\alpha,\beta)^{1/1-\alpha}\left(1+\left(\frac{2}{\alpha}\left(1-\left(\frac{1}{f_N}\right)^{1/1-\alpha}\right)\right)^{1/2}\right). \quad (36)$$

The similarity to the CAK case (Eq. 24) is striking. Since $v_c^2 \ll v_\infty^2$, the main difference lies in the integral. In the CAK case we have $Z(u,\alpha,\beta)\equiv 1$, because of $f(u,\alpha,\beta)\equiv 1$. In the finite cone angle case, however, $Z(u,\alpha,\beta)$ has the following properties:

(i) $Z(u,\alpha,\beta)$ increases monotonically from $u=1$ until $u=1/(2(1+\beta))$, since f_N increases in this interval.

$$Z(1,\alpha,\beta)=1$$

$$Z\left(\frac{1}{1+\beta},\alpha,\beta\right) = (1+\alpha)^{1/1-\alpha}\left(1+\left(\frac{2}{\alpha}\left(1-\left(\frac{1}{1+\alpha}\right)^{1/1-\alpha}\right)\right)^{1/2}\right)$$

$$Z\left(\frac{1}{2(1+\beta)},\alpha,\beta\right) \approx (1+\alpha)(1+\zeta) \times\left(1+\left(\frac{2}{\alpha}\left(1-\left(\frac{1}{1+\alpha}\right)^{1/1-\alpha}\frac{1}{1+\zeta}\right)\right)^{1/2}\right)$$

$$\zeta = \frac{1}{8}\frac{\alpha}{1-\alpha}\frac{1}{\beta(\beta+1)} \quad (37a)$$

(ii) $Z(u,\alpha,\beta)$ decreases from $u=1/(2(1+\beta))$ until $u=0$. We have

$$Z(0,\alpha,\beta) = Z\left(\frac{1}{1+\beta},\alpha,\beta\right). \quad (37b)$$

(see also the discussion in the Appendix).

Typical examples for $Z(u,\alpha,\beta)$ are plotted in Fig. 3. It is evident that Z becomes much larger than unity with decreasing reciprocal radius $u=1/x$. Therefore, much higher velocities are obtained than in the CAK case. Physically, $Z>1$ reflects the fact that $\dot{M}$ is smaller than in the CAK case. Thus, the constant C in the equation of motion (Eq. 5) is larger in the finite cone angle case, because the radiative acceleration is the radiative force divided by the lower finite cone angle density. The integral

$$I(\alpha,\beta) = \int_0^1 Z(u,\alpha,\beta)\,du \quad (38)$$

then describes, how much the terminal velocity is increased in the finite cone angle case:

$$v_\infty = v_\infty^{CAK}\, I(\alpha,\beta)^{1/2}. \quad (39)$$

(v_∞^{CAK} is given by Eq. (25)). Table 1 gives the results of the numerical integration of Eq. (38).

We see that $I(\alpha,\beta)$ depends strongly on α, whereas the influence of β, in particular for the more realistic domain of $0.7\le\beta\le 1.0$, is rather small, as was already to be expected from Fig. 3. The least square fit procedure of FA to their numerical results suggests that $I(\alpha,\beta)\sim\alpha/(1-\alpha)$. Figure 4 shows that this is a good approximation, in particular for $\beta=1$. From Fig. 6 for the case $\delta=0$ we conclude in addition that v_∞/v_{esc} agrees well with the values given by FA (their Fig. 8, high v_{esc}). A more detailed analytical approximation of $Z(u,\alpha,\beta)$ and $I(\alpha,\beta)$ will be given below together with detailed comparisons with numerical calculations.

4.2. *The role of δ*

As mentioned above, the factor $(n_E/W)^\delta$ in the force multiplier (see Eq. (2)) takes into account the changes of ionization when going outward in the wind. We now investigate the influence of

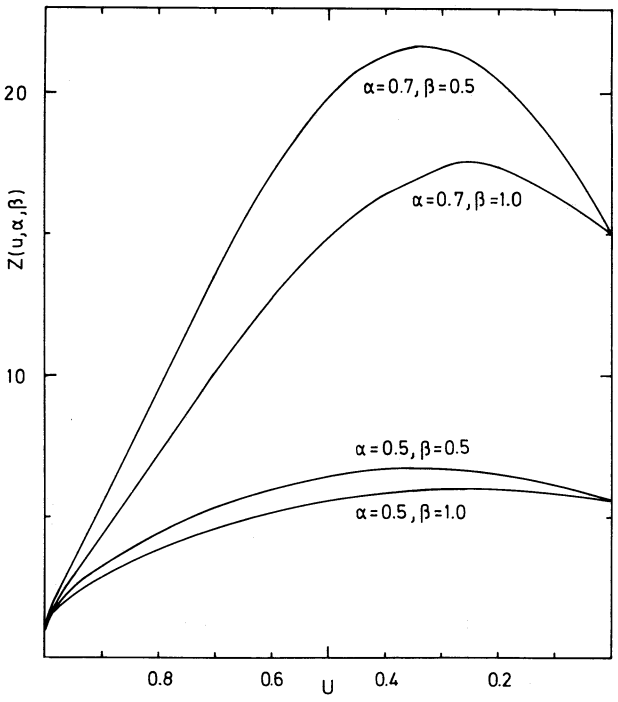

Fig. 3. The function $Z(u,\alpha,\beta)$ for different parameters α and β

Table 1. The integral $I(\alpha, \beta)$

β \ α	0.5	0.6	0.7
0.5	5.55	8.21	15.60
0.7	5.22	7.54	13.79
1.0	4.96	7.05	12.51
∞	4.34	5.91	9.82

this factor on the wind dynamics. For this purpose we have to approximate the run $n_E(x)$ of electron density in the wind. This is done by an approximation for the velocity field, which is similar as Eq. (13) but avoids the singularity at $x=1$ for $n_E \sim 1/(x^2 v)$:

$$v(x) = v_\infty((1 - v_1/v_\infty)(1 - 1/x)^\beta + v_1/v_\infty). \tag{40}$$

Using the mass conservation, we obtain then

$$\left(\frac{n_E}{W}\right)^\delta = g(u, \delta, \beta) = \Delta\left(\frac{1}{u^2}\left((1-u)^\beta + \frac{v_1}{v_\infty}\right)(1-(1-u^2)^{1/2})\right)^{-\delta}$$

$$\Delta = \left(\frac{\dot{M}}{4\pi R_*^2 v_\infty}\frac{2}{m_H}\frac{1 + I_{He} Y_{He}}{1 + 4Y_{He}} \times 10^{-11}\ \mathrm{cm}^3\right)^\delta \tag{41}$$

(for definition of I_{He}, Y_{He}, m_H see PPK Eq. (27)).

Because of the limited range of δ between 0.0 and 0.1 $g(u, \delta, \beta)$ can be approximated in a much simpler way as demonstrated by Fig. 5:

$$g(u, \delta, \beta) \approx \Delta 2^\delta (q(\delta, \beta) u^2 + 1)$$

$$\begin{aligned} q(\delta, \beta) &= 22.5^\delta - 1, && \beta = 2 \\ &= 7.5^\delta - 1, && \beta = 1 \\ &= 4.0^\delta - 1, && \beta = 0.7 \\ &= 2.5^\delta - 1, && \beta = 0.5 \\ &= 1.18^\delta - 1, && \beta = 0.25 \end{aligned} \tag{42}$$

For reason of simplicity we will use for the rest of this paper Eq. (42) for $g(u, \delta, \beta)$. The force multiplier function f then becomes

$$f(x, \alpha, \beta, \delta) = CF(x, \alpha, \beta)\, g(x, \delta, \beta). \tag{43}$$

The same procedure as in Sect. 1, then yields

$$C = \frac{1}{f(1, \alpha, \beta, \delta)}\frac{1}{\alpha}\left(\frac{\alpha}{1-\alpha}\right)^{1-\alpha} A^{1-\alpha} \tag{44}$$

for the eigenvalue C. For the velocity we obtain

$$v^2(u) = v_c^2 + \frac{\alpha}{1-\alpha} v_{esc}^2 \int_u^1 Z(u, \alpha, \beta, \delta)\, du \tag{45a}$$

$$Z(u, \alpha, \beta, \delta) = f_N(u, \alpha, \beta, \delta)^{1/1-\alpha} \times \left(1 + \left(\frac{2}{\alpha}\left(1 - \left(\frac{1}{f_N(u, \alpha, \beta, \delta)}\right)^{1/1-\alpha}\right)\right)^{1/2}\right) \tag{45b}$$

$$f_N(u, \alpha, \beta, \delta) = f(u, \alpha, \beta, \delta)/f(1, \alpha, \beta, \delta). \tag{45c}$$

The effects of δ on the terminal velocity v_∞ are demonstrated in Fig. 6, where the square root of

$$I(\alpha, \beta, \delta) = \int_0^1 Z(u, \alpha, \beta, \delta)\, du \tag{46}$$

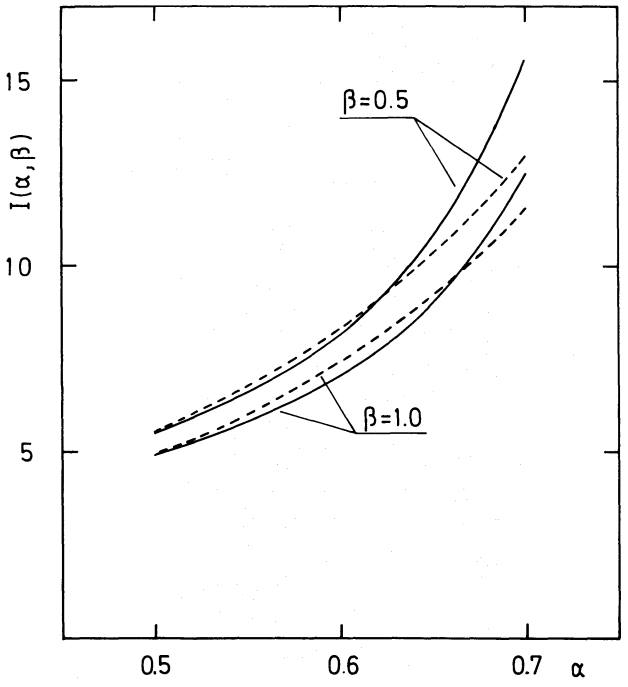

Fig. 4. The integral $I(\alpha, \beta)$ (fully drawn) compared with $I(\alpha, \beta) = I(0.5, \beta)\, \alpha/(1-\alpha)$ (dashed)

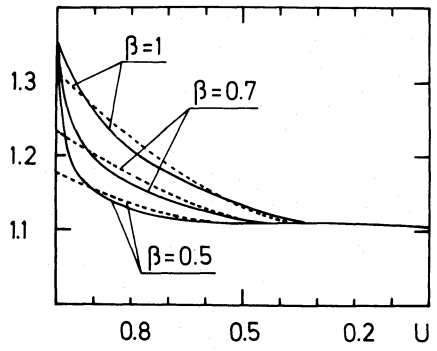

Fig. 5. The function $g(u, \delta, \beta)/\Delta$ for $v_1/v_\infty = 0.05$ and $\delta = 0.1$ and different values of β (fully drawn) compared with the approximation of Eq. (42) (dotted)

multiplied by $\alpha/(1-\alpha)$ is plotted. (note that we normally have $v_c \ll v_\infty$). We see that an increase of δ decreases the terminal velocity significantly. This was to be expected, since $(n_E/W)^\delta$ is decreasing with increasing x. This means that the increase of the line force due to the finite cone angle effect is damped partially by the change of the ionization structure. Thus, both parameters α and δ are important for the terminal velocity.

Adopting $v_\infty \approx v_{esc}(\alpha/1-\alpha)^{1/2} I(\alpha, \beta, \delta)^{1/2}$ we obtain from Eqs. (10), (41), (44) the mass-loss rate for $\delta = 0$

$$\dot{M} = (DI(\alpha, \beta, \delta)^{-1/2})^{\delta/\alpha - \delta}\left(\frac{1+q}{1+\alpha}\right)^{1/\alpha - \delta} \dot{M}_{CAK}^{\alpha/\alpha - \delta}$$

$$D = \frac{4}{m_H}\frac{1 + I_{He} Y_{He}}{1 + 4Y_{He}}\frac{1}{4\pi R_*^2 v_{esc}}\left(\frac{1-\alpha}{\alpha}\right)^{1/2} * 10^{-11}\ \mathrm{cm}^3. \tag{47}$$

Table 2 shows the influence of δ on the mass-loss rate for typical O-stars and a Central Star ($k = 0.1$, $\alpha = 0.7$, $\beta = 1.0$ were

chosen). Obviously, an increase of δ from 0.0 to 0.1 can increase the mass-loss rate up to 50%. While this effect might be only marginally observable, it is clearly of importance if radiation driven wind mass-loss rates are incorporated into stellar evolution codes, where changes of $\dot{M}$ of that order have significant effects.

4.3. Simple analytical approximations

Although the integrals in Eqs. (45) and (46) can be easily evaluated numerically, we give in this subsection a simple approximation of $Z(u, \alpha, \beta, \delta)$, which allows the analytical calculation of $I(\alpha, \beta, \delta)$. In this way a direct formula for $v_\infty/v_{\rm esc}$ can be given.

As shown in Appendix 1, a sufficient accurate approximation for $CF^{1/1-\alpha}$ is

$$CF(u,\alpha,\beta)^{1/1-\alpha} \approx 1+b_1u-b_2u^2,\ 0\le u\le\frac{1}{1+\beta}$$

$$\approx a_0-a_1u,\ \frac{1}{1+\beta}\le u\le 1 \tag{48}$$

$$b_1=\frac{1}{2}\frac{\alpha}{1-\alpha}\frac{1}{\beta};\ b_2=\frac{1}{2}\frac{\alpha}{1-\alpha}\frac{\beta+1}{\beta};$$

$$a_0=\frac{1}{\beta}\left(1+\beta-\left(\frac{1}{1+\alpha}\right)^{1/1-\alpha}\right);\ a_1=\frac{1+\beta}{\beta}\left(1-\left(\frac{1}{1+\alpha}\right)^{1/1-\alpha}\right).$$

On the other hand, because of $q(\delta,\beta)u^2 \ll 1$ we can approximate

$$g(u,\delta,\beta)^{1/1-\alpha}\approx(\Delta 2^\delta)^{1/1-\alpha}\left(1+\frac{1}{1-\alpha}qu^2\right). \tag{49}$$

Thus, the first factor in Eq. (45b) for $Z(u, \alpha, \beta, \delta)$ can be given in a simple form. We now still need an expansion of the square root. In the Appendix and Fig. 17 it is demonstrated that this is a rapidly increasing function with u, which can be approximated by

$$F(u,\alpha,\beta,\delta)=\left(\frac{2}{\alpha}\left(1-\left(\frac{1}{f_{\rm N}(u,\alpha,\beta,\delta)}\right)^{1/1-\alpha}\right)\right)^{1/2}$$

$$\approx F_0(\alpha,\beta,\delta)(1-u^7(1-u+u^9))$$

$$F_0=\left(\frac{2}{\alpha}\left(1-\left(\frac{1}{f_{\rm N}(0,\alpha,\beta,\delta)}\right)^{1/1-\alpha}\right)\right)^{1/2}. \tag{50}$$

This means that in total $Z(u, \alpha, \beta, \delta)$ can be approximated by

$$Z(u,\alpha,\beta,\delta)\approx Z_0(a_0-a_1u)\left(1+\frac{1}{1-\alpha}qu^2\right)$$

$$\times\left(1+\frac{F_0}{F_0+1}(u^8-u^7-u^{16})\right),\ \frac{1}{1+\beta}\le u\le 1$$

$$\approx Z_0(1+b_1u-b_2u^2)\left(1+\frac{1}{1-\alpha}qu^2\right)$$

$$\times\left(1+\frac{F_0}{F_0+1}(u^8-u^7-u^{16})\right),\ 0\le u\le\frac{1}{1+\beta}$$

$$Z_0(\alpha,\beta,\delta)=Z(0,\alpha,\beta,\delta)=\left(\frac{1+\alpha}{1+q}\right)^{1/1-\alpha}(1+F_0). \tag{51}$$

For the approximation of the integral $I(\alpha, \beta, \delta)$ (Eq. 46) the terms involving $F_0/(F_0+1)$ give only a 5% contribution, which is of the order of the accuracy of the approximation for $Z(u, \alpha, \beta, \delta)$ itself.

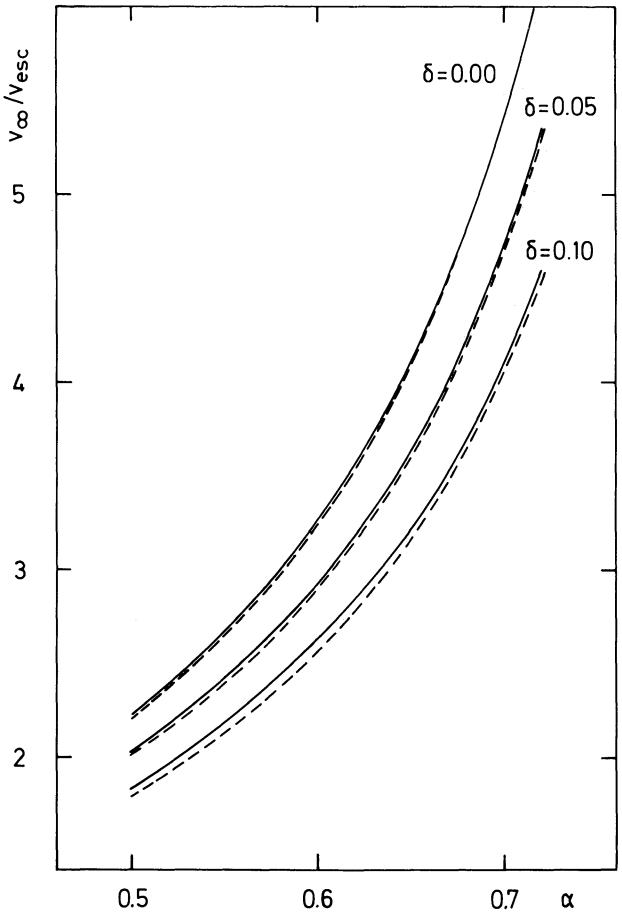

Fig. 6. The effect of δ on $v_\infty/v_{\rm esc}$ computed according to Eq. (46). The dashed curves show the corresponding approximation given by Eq. (52). ($\beta=1$ was chosen)

We thus neglect these terms for simplicity and obtain

$$I(\alpha,\beta,\delta)\approx Z_0\left(a_0\left(\left(1-\frac{1}{1+\beta}\right)+\frac{1}{1-\alpha}\frac{q}{3}\left(1-\left(\frac{1}{1+\beta}\right)^3\right)\right)\right.$$

$$-a_1\left(\frac{1}{2}\left(1-\left(\frac{1}{1+\beta}\right)^2+\frac{1}{1-\alpha}\frac{q}{4}\left(1-\left(\frac{1}{1+\beta}\right)^4\right)\right)\right)$$

$$+\frac{1}{1+\beta}+b_1\left(\frac{1}{2}\left(\frac{1}{1+\beta}\right)^2+\frac{1}{4}\frac{1}{1-\alpha}q\left(\frac{1}{1+\beta}\right)^4\right)$$

$$-b_2\left(\frac{1}{3}\left(\frac{1}{1+\beta}\right)^3+\frac{1}{1-\alpha}\frac{q}{5}\left(\frac{1}{1+\beta}\right)^5\right)$$

$$\left.+\frac{1}{3}\frac{1}{1-\alpha}q\left(\frac{1}{1+\alpha}\right)^3\right). \tag{52}$$

Figure 6 shows that this approximation is sufficiently accurate.

5. Finite cone angle effects of winds above geometrically extended photospheres

We now consider the fact that the coordinate x_c of the critical point increases with $v_s^2/v_{\rm esc}^2=\Delta r/R_*$. Figure 7 shows the corresponding results of fully numerical finite cone angle calculations carried out with $\alpha=0.709$, $\delta=0.05$ for Central Stars of PN (see

Table 2. Influence of δ on $\dot{M}$

Typical O5V-star: $T_{\rm eff}=45000$ K, $\log g=4.0$, $R/R_\odot=12$

δ	$\dot{M}$ in $10^{-6}\,M_\odot$/yr
0.0	2.07
0.05	2.33
0.1	2.73

Typical central star: $T_{\rm eff}=45000$ K, $\log g=4.2$, $R/R_\odot=1.0$

δ	$\dot{M}$ in $10^{-8}\,M_\odot$/yr
0.0	1.33
0.05	1.61
0.10	2.08

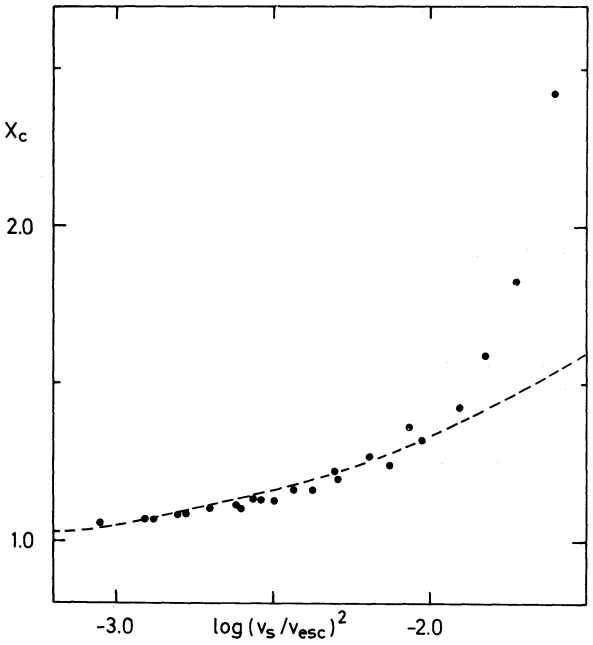

Fig. 7. The coordinate x_c of the critical point as function of $\log(v_s^2/v_{esc}^2)$ for detailed numerical finite cone angle calculations for Central Stars of PN (see text). The dashed curve corresponds to the approximation given by Eq. (58)

Paper V. This effect has also been mentioned in the paper by FA). In the first step, we want to derive the numerically observed correlation of Fig. 7 as an approximative result of the singularity condition (Eq. 11), the regularity condition (Eq. 12) and the equation of motion (Eq. 5). For the function $f(x, \alpha, \beta, \delta)$ Eq. (43) and (15) are used. The procedure is analogous to Sect. 3 for the case $f\equiv 1$. The singularity condition yields again the same result as Eq. (21), however Eq. (20) has to be replaced by

$$C=\frac{1-v_s^2/v_c^2}{\alpha f(x_c, \alpha, \beta, \delta)}\, y_c^{1-\alpha}. \tag{53}$$

The regularity condition yields

$$\frac{1-4\,v_s^2 x_c/v_{esc}^2}{1-\alpha}\,\frac{f'}{f}+\frac{4\,v_s^2}{v_{esc}^2}=\frac{v_{esc}^2\,v_s^2}{x_c^2\,v_c^4}\left(\frac{\alpha}{1-\alpha}\right)^2\left(\frac{1-4\,v_s^2\,x_c/v_{esc}^2}{1-v_s^2/v_c^2}\right)^2. \tag{54a}$$

(Note that (54a) and (22) are identical, if $d/dx(f)=f'=0$). Assuming again $v_s^2/v_c^2\ll 1$ and $4v_s^2\,x_c/v_{esc}^2\ll 1$ we obtain

$$\frac{1}{1-\alpha}\,\frac{f'}{f}+\frac{4\,v_s^2}{v_{esc}^2}=\left(\frac{\alpha}{1-\alpha}\right)^2\frac{v_{esc}^2\,v_s^2}{x_c^2\,v_c^4}. \tag{54b}$$

Equation (54b) involves two problems. The presence of f'/f modifies it relative to the CAK-case. However, since f'/f can be given as a function of x, we can take this into account. In addition, an estimate for v_c is again needed. However, since now the finite cone correction factor leads to the varying function $f(x, \alpha, \beta, \delta)$ in the equation of motion (Eq. 5), Eq. (23) does not hold anymore, since $y_0(x)$ is not constant. Thus, the estimate of v_c has to be modified relative to the CAK-case: Since $f(x, \alpha, \beta, \delta)$ is monotonically decreasing in the interval $1+\beta\geq x\geq 1$, a solution of Eq. (5) can only be found inward of the critical point x_c, if x_c is already close enough to the sonic point x_s so that the decrease in $f(x, \alpha, \beta, \delta)$ is compensated by the decrease of the slope of $A+y\,(1-v_s^2/v^2)$ (see Fig. 8). Thus, x_c in the finite cone angle case must be much closer to x_s and to $x=1$ as in the CAK case (see also PPK).

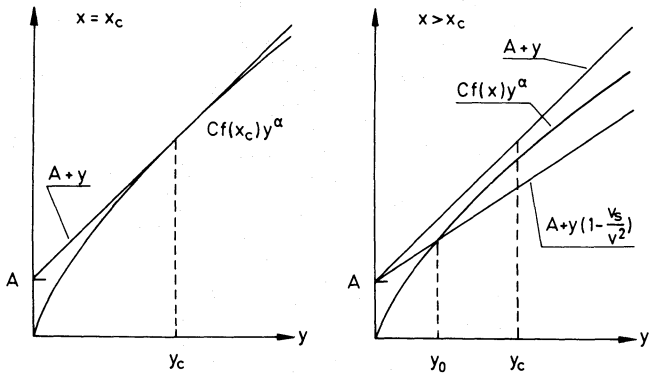

Fig. 8. Sketch of the solution $y_0(x)$ for $x<x_c$ in the finite cone angle case

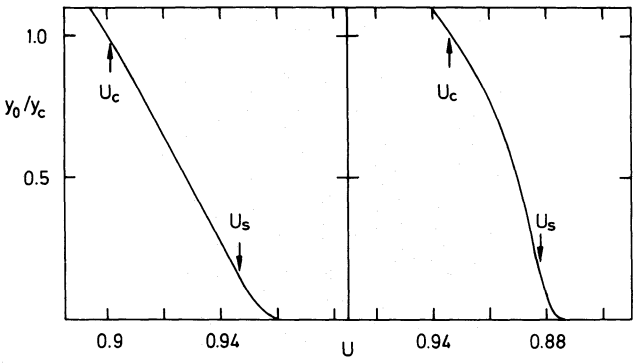

Fig. 9. y_0/y_c as function of reciprocal radius $u=1/x$ for two numerical finite cone wind models of Central Stars of Planetary Nebulae (left: $M/M_\odot=0.565$, $T_{\rm eff}=60000$K, $\log L/L_\odot=3.53$; right: $M/M_\odot=0.546$, $T_{\rm eff}=80000$K, $\log L/L_\odot=2.99$). The sonic u_s and the critical point u_c are indicated

Generally, all the wind models we have calculated so far show a roughly linear slope of y_o versus the reciprocal radius $u=1/x$ (Fig. 9 shows the behaviour of $y_0(u)$ for two examples. Figure 10 sketches the general behaviour of $y_0(u)$ in the CAK and the finite cone angle case). Using Eq. (19b) (and $v_s^2/v_c^2 \ll 1$) this leads to

$$v_c^2=\frac{2}{R_*}\int_{u_c}^{u_s} y\,du=\frac{1}{R_*}\frac{y_c^2}{x_c^2}\frac{y_c^2}{y'(x_c)}\left(1-\frac{y_s^2}{y_c^2}\right). \tag{55}$$

As shown in Appendix 2, a sufficient accurate approximation of Eq. (55) is

$$v_c=v_s(\varphi(v_s/v_{esc})/(1-\alpha))^{1/2}$$

$$\varphi(v_s/v_{esc})=3.(v_s/v_{esc})^{0.3(0.36+\log(v_s/v_{esc}))} \tag{55a}$$

Figure 11 shows that this is a sufficiently good approximation as long as v_s/v_{esc} and, consequently, x_c are not too small so that the approximations for the velocity field (Eq. (13) and/or Eq. (40)), which enter into our algorithm, do not become totally invalid. In these cases (typical objects are marked by crosses in Fig. 11) it is not possible to determine x_c and v_c accurately enough by our method. However, fortunately, just in these cases x_c approaches a constant value of 1.03, as we have found by the fully correct numerical treatment of the problem. In addition, v_c^2 becomes very small compared with v_∞^2 so that the accuracy of v_c is not important for the calculation of v_∞ (see Eq. (19) or (36)). Thus, we adopt a minimum value of $x_c^{min}=1.03$ and develop a formula for the more extended atmosphere with $x_c>1.03$. For this purpose we insert Eq. (55a) into (54b) and obtain

$$\frac{v_{esc}^2}{v_s^2}\frac{\alpha^2(1-\alpha)}{\varphi^2}=x_c^2 f'/f. \tag{56}$$

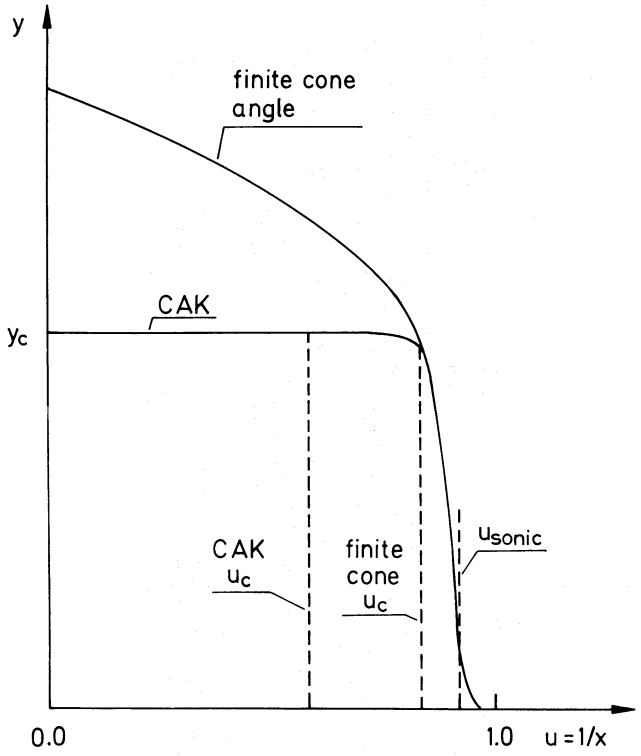

Fig. 10. The general behaviour of $y_0(u)$ in the finite cone angle and in the CAK case

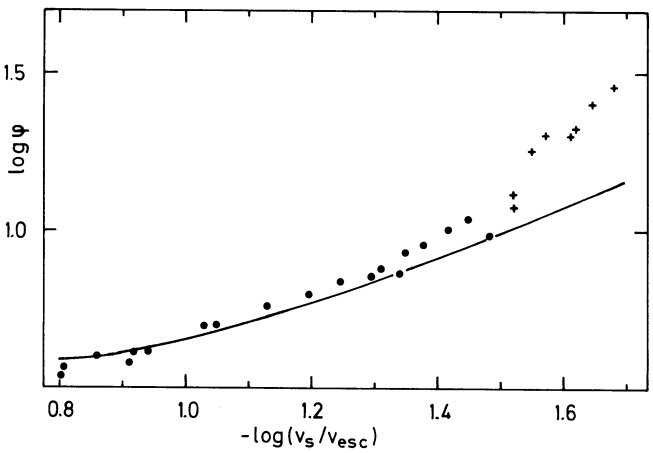

Fig. 11. log φ as function of log v_s/v_{esc} (dots: results of detailed numerical calculations, crosses: see text, fully drawn: the approximation given by Eq. (55a))

Since the right hand side of Eq. (56) is a known function, which is fairly well approximated by (see Fig. 12)

$$x_c^2 f'/f=\alpha^{3/5}(\alpha+1)1.46/x_c^3-2q_c/x_c. \tag{57}$$

x_c can be determined by an approximate use of Cardan's formula as function of v_{esc}^2/v_s^2, α and δ

$$x_c=(\alpha^{3/5}(\alpha+1)\times 1.46/\sigma)^{1/3}-\frac{2}{3}q_c/\sigma, \quad \text{for} \quad x_c\geq 1.03$$

$$\sigma=\frac{v_{esc}^2\,\alpha^2(1-\alpha)}{v_s^2\,\varphi^2}, \tag{58a}$$

where $q_c(\delta, \beta_c)$ is defined in the same way as q in Eq. (42). However, since close to the critical point the exponent describing the velocity field in Eq. (40) tends to change drastically, an extra value β_c has to be chosen to calculate q_c at the critical point. These values are given in Table 3.

If formula (58a) yields values for x_c smaller than 1.03, we adopt

$$x_c=1.03. \tag{58b}$$

Figure 7 shows this approximation to be valid for not too large x_c as long as the previous assumption

$$4v_s^2\,x_c/v_{esc}^2 \ll 1$$

is not violated.

With these expressions for x_c and v_c we have now boundary values for the integral of Eq. (19). In the next step we calculate $y_0(x)$ for $x>x_c$ in the same way as in Sect. 4. The result is

$$y_0(u)\approx Z(u,\alpha,\beta,\delta,u_c)=f_N(u,\alpha,\beta,\delta,u_c)^{1/1-\alpha}$$

$$\times\left(1+\left(\frac{2}{\alpha}\left(1-\left(\frac{1}{f_N(u,\alpha,\beta,\delta,u_c)}\right)^{1/1-\alpha}\right)\right)^{1/2}\right)$$

$$f_N(u,\alpha,\beta,\delta,u_c)=\frac{f(u,\alpha,\beta,\delta)}{f(u_c,\alpha,\beta,\delta)}, \tag{59}$$

where f is given by Eq. (43). Using the same approximations for $f(u,\alpha,\beta,\delta)$ and the square root in Eq. (59) as in Sect. 4 we can then

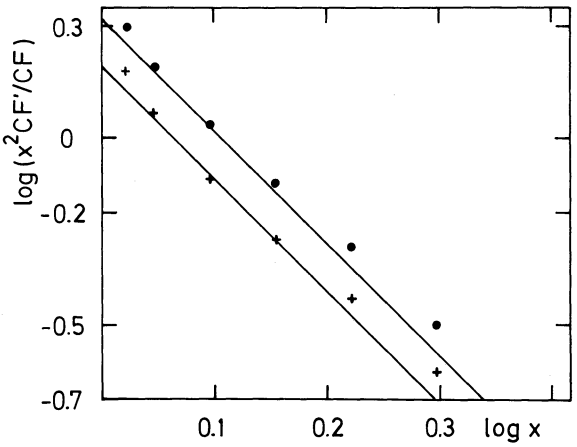

Fig. 12. Logarithm of the function x^2CF'/CF for $\beta=1.0$, $\alpha=0.7$ (dots) and $\beta=1.0$, $\alpha=0.5$ (crosses). The approximation of Eq. (57) is also shown (fully drawn)

Table 3. β_c as function of α and δ

0.01	$\delta<.03\leq$	$\delta<.055\leq$	$\delta<.085\leq$	$\delta<.095\leq$	δ
$0.7<\alpha$	2.0	2.0	1.0	1.0	0.7
$0.7\geq\alpha$	2.0	1.0	0.7	0.5	0.25

compute the velocity field according to Eq. (19).

$$\left(\frac{v_\infty}{v_{esc}}\right)^2=\frac{\alpha}{1-\alpha}\left(\frac{1-\alpha}{\alpha}\left(\frac{v_c}{v_{esc}}\right)^2\right.$$
$$+Z_0\left(\int_0^{1/1+\beta}(1+b_1u-b_2u^2)\left(1+\frac{1}{1-\alpha}qu^2\right)du\right.$$
$$\left.\left.+\int_{1/1+\beta}^{u_c}(a_0-a_1u)\left(1+\frac{1}{1-\alpha}qu^2\right)du\right)\right)$$
$$=\frac{\alpha}{1-\alpha}\left(\frac{1-\alpha}{\alpha}\left(\frac{v_c}{v_{esc}}\right)^2\right.$$
$$+Z_0\left(a_0\left(u_c-\frac{1}{1+\beta}+\frac{1}{1-\alpha}\frac{q}{3}\left(u_c^3-\left(\frac{1}{1+\beta}\right)^3\right)\right)\right.$$
$$\left.-a_1\left(\frac{1}{2}\left(u_c^2-\left(\frac{1}{1+\beta}\right)^2\right)+\frac{1}{1-\alpha}\frac{q}{4}\left(u_c^4-\left(\frac{1}{1+\beta}\right)^4\right)\right)\right)$$
$$+\frac{1}{1+\beta}+b_1\left(\frac{1}{1+\beta}\right)^2\left(\frac{1}{6}+\frac{1}{20}\frac{q}{1-\alpha}\left(\frac{1}{1+\beta}\right)^2\right)$$
$$\left.+\frac{1}{3}\frac{1}{1-\alpha}q\left(\frac{1}{1+\beta}\right)^3\right)=\frac{\alpha}{1-\alpha}I(\alpha,\beta,\delta,u_c)$$

$$Z_0(\alpha,\beta,\delta,u_c)=G\left(1+\left(\frac{2}{\alpha}\left(1-\frac{1}{G}\right)\right)^{1/2}\right)$$

$$G(\alpha,\beta,\delta,u_c)=(a_0-a_1u_c)^{-1}(qu_c^2+1)^{1/\alpha-1}.' \qquad (60)$$

The mass-loss rate is given by

$$\dot M=(DI(\alpha,\beta,\delta,u_c)^{-1/2})^{\delta/\alpha-\delta}(CF(u_c)(1+qu_c^2))^{1/\alpha-\delta}\dot M_{CAK}^{\alpha/\alpha-\delta}. \qquad (61)$$

Formulae (60) and (61) now allow one to compute directly v_∞ and $\dot M$, if the stellar parameters M_*, R_*, L are specified and the force multiplier parameters k, α, δ are known. β is a free parameter, which was introduced to describe the influence of the velocity gradient on the finite cone angle function f for layers clearly above the critical point. The influence of this parameter, which when compared with detailed numerical solutions of the radiation driven wind equations lies between 0.7 and 1.0 (see also PPK), on v_∞ and $\dot M$ is small. We, therefore, adopt $\beta=1.0$ in the following comparison with numerical results.

6. The cooking recipe for $\dot M$ and v_∞

In the foregoing sections we have developed an approximate algorithm to solve the equation of motion and the eigenvalue problem of radiation driven winds including the finite cone angle effect. Since this was done in several more or less complicated steps, we summarize in this section the basic steps for those who simply want to apply the approximate formulae for $\dot M$ and v_∞. Six parameters have to be specified: Stellar luminosity L, stellar mass M_* and effective temperature T_{eff} plus the force multiplier parameters k, α, δ. For the stellar parameters other equivalent parameters (T_{eff}, log g, R_*, for instance) can be used as well. For the force multiplier parameters either the old rather inaccurate values by Pauldrach et al. (1986) or Kudritzki et al. (1987) or Abbott (1982) can be used for rough estimates. The very recent work described in Sect. 1, which combines full multilevel NLTE of all the 133 ions driving the wind with the radiation driven wind hydrodynamics, yields much better k, α, δ. For stars like ζ Puppis values can be found in Pauldrach (1987) and Puls (1987). For Central Stars of Planetary Nebulae k, α, δ values are given by Pauldrach et al. (1988). For galactic O-stars evolving with 40, 60, 80 and 120 $M_\odot$ away from the ZAMS new force multiplier parameters have also been calculated very recently (Pauldrach et al., 1989). In future work, we will continue to calculate data for other groups of stars.

The first step is to calculate x_c, the coordinate of the critical point and the critical velocity v_c using Eq. (55a) and (58a) or (58b) and the β_c values of Table 3. (Note that v_{esc} as defined by Eq. (7) includes the factor $(1-\Gamma)$, see below). Now we apply Eq. (60) for $\beta=1$ to calculate v_∞/v_{esc}, which yields

$$\frac{v_\infty^2}{v_{esc}^2}=\frac{\alpha}{1-\alpha}I(\alpha,1,\delta,u_c)$$

$$I(\alpha,1,\delta,u_c)=\frac{1-\alpha}{\alpha}\left(\frac{v_c}{v_{esc}}\right)^2+Z_0\left(a_0\left(u_c-\frac{1}{2}+\frac{q}{1-\alpha}\frac{1}{3}\left(u_c^3-\frac{1}{8}\right)\right)\right.$$
$$\left.-a_1\left(\frac{1}{2}\left(u_c^2-\frac{1}{4}\right)+\frac{q}{1-\alpha}\frac{1}{4}\left(u_c^4-\frac{1}{16}\right)\right)\right)$$
$$+\frac{1}{2}+\frac{1}{8}\frac{\alpha}{1-\alpha}\left(\frac{1}{6}+\frac{1}{80}\frac{q}{1-\alpha}\right)+\frac{1}{24}\frac{q}{1-\alpha} \qquad (62)$$

Z_0, G, u_c, q are defined as follows

$$u_c=x_c^{-1},\ q=7.5^\delta-1$$
$$a_0=2-\left(\frac{1}{1+\alpha}\right)^{1/(1-\alpha)},\ a_1=2\left(1-\left(\frac{1}{1+\alpha}\right)^{1/(1-\alpha)}\right) \qquad (63)$$
$$Z_0=G\left(1+\left(\frac{2}{\alpha}\left(1-\frac{1}{G}\right)\right)^{1/2}\right)$$
$$G=(a_0-a_1u_c)^{-1}(qu_c^2+1)^{1/\alpha-1}. \qquad (64)$$

$I(\alpha, 1, \delta, u_c)$ as defined by Eq. (62) can then also be used to calculate the mass-loss rate $\dot{M}$

$$\dot{M} = (DI(\alpha, 1, \delta, u_c)^{-1/2})^{\delta/(\alpha-\delta)} (CF(u_c, \alpha, 1) \times (1+qu_c^2)^{1/\alpha-\delta}) \dot{M}_{CAK}^{\alpha/(\alpha-\delta)} \quad (65)$$

The CAK mass-loss rate $\dot{M}_{CAK}$ is given by Eq. (27). Note that v_{th} in this Eq. is the thermal velocity of the protons and that σ_E and Γ are calculated by

$$\sigma_E = 0.398 \frac{1+I_{He}\,Y}{1+4Y}$$

$$\Gamma = 7.66\,10^{-5}\,\sigma_E \frac{L/L_\odot}{M/M_\odot}, \quad (65)$$

where I_{He} is the number of electrons provided per helium nucleus ($I_{He}=2$ for O-stars) and $Y=N_{He}/N_H$. In the same way the sound velocity v_s, which is needed for the determination of x_c (Eq. 55a) is calculated

$$v_s = 9.085\,10^3 \left(\frac{2+(1+I_{He})\,Y\,T_{eff}}{1+4Y}\right)^{1/2}. \quad (67)$$

The constant D is given by Eq. (47) and $CF(u_c, \alpha, 1)$, the finite cone angle correction factor for $\beta=1$ at the critical point, is given by

$$CF(u_c, \alpha, 1) = \frac{1}{\alpha+1}\frac{1}{\lambda_c}(1-(1-\lambda_c)^{1+\alpha})$$

$$\lambda_c = u_c^2\left(2-\frac{1}{u_c}\right). \quad (68)$$

(Note that $CF(1/2, \alpha, 1)=1$.)

Equations (62) and (64) allow the easy computation of v_∞ and $\dot{M}$ as function of stellar parameters for given force multiplier parameters k, α, δ. A sample of small FORTRAN subroutines for that purpose can be provided upon request.

7. Comparison with numerical solutions of the wind equations

The accuracy of our approximative solutions has to be tested by comparison with the numerical integration of the wind equations (for a description of the numerical procedure see PPK). We will do this for two cases: Massive O-stars and Central Stars of PN. As approximative formulae for v_∞ and $\dot{M}$ we use Eqs. (62) and (64) as described in Sect. 6.

7.1. Massive O-stars

A comprehensive grid of wind models along evolutionary tracks has been computed by Kudritzki et al. (1987). A comparison of these computations with Eq. (62) for v_∞ as function of v_{esc} is given in Fig. 13. Figure 14 shows the corresponding comparison of $\dot{M}$ as function of luminosity (compare also with Figs. 3 and 5 of Kudritzki et al.). We see that the agreement is within 5% for v_∞ and within 10% for $\dot{M}$. The approximative values for $\dot{M}$ are systematically a little too small. This could be overcome by choosing $\beta \approx 1.5$ for the computation of $\dot{M}$. Physically, this represents the well known fact that the velocity field around the critical point is represented by a different exponent β than the layers above the critical point. However, in view of the small percentage of the discrepancies we regard Eq. (62) and (63) as accurate enough.

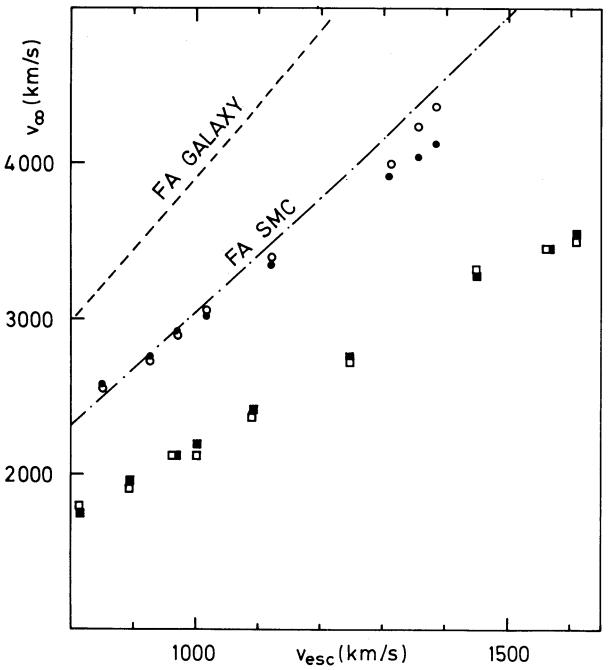

Fig. 13. v_∞ as function of v_{esc} for massive O-stars. Open circles and squares represent detailed numerical calculations for the Galaxy ($\alpha=0.64$, $\delta=0.07$) and the SMC ($\alpha=0.58$, $\delta=0.104$) (see Kudritzki et al., 1987). Filled circles and squares represent the results obtained with the approximation of Eq. (62). The dashed and dashed-dotted curves correspond to the formula by Friend and Abbott (1986)

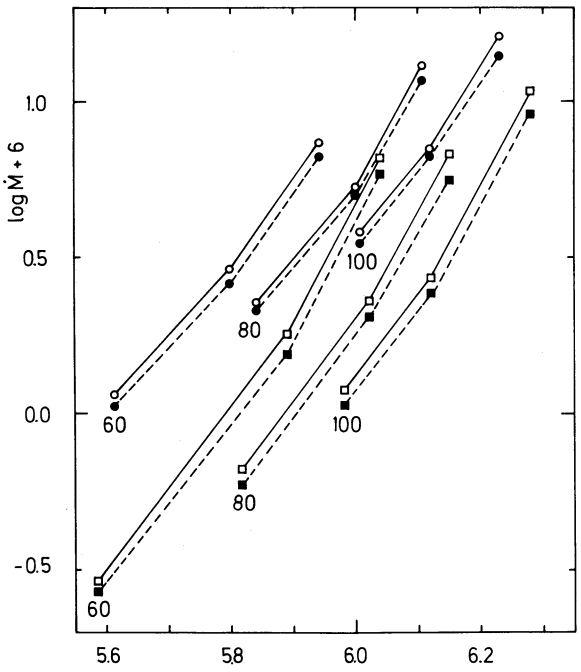

Fig. 14. $\dot{M}$ as function of $\log L/L_\odot$ along evolutionary tracks labelled by their mass in solar units (fully drawn: numerical calculations; dashed: Eq. (63)) (see also Kudritzki et al., 1987). Circles: galactic O-stars ($k=0.124$, $\alpha=0.64$, $\delta=0.07$); squares: SMC O-stars ($k=0.097$, $\alpha=0.580$, $\delta=0.104$)

The relation $v_\infty = (\alpha/1-\alpha)\,2.2 * v_{esc} * (v_{esc}/1000\ \mathrm{km\,s^{-1}})^{0.2}$ as found by FA is also shown in Fig. 13. Since this relation neglects the influence of δ, its results must differ from the results displayed in Fig. 13, as is already indicated by Fig. 6.

7.2. *Central stars of PN*

While the effects of spherical photospheric extension are moderate for massive O-stars, they become important for Central Stars of Planetary Nebulae (CSPN). Recently, Pauldrach et al. (1988, Paper V) have computed detailed wind models for CSPN of different mass between 0.55 $\dot{M}_\odot$ to 1.0 $\dot{M}_\odot$ evolving at almost constant luminosity towards higher temperature. In Fig. 15 we show the results of a sequence of models, which were all calculated with $\alpha = 0.709$ and $\delta = 0.051$. We see that v_∞ and $\dot{M}$ are well approximated by Eqs. (62) and (64) for all the tracks. Figure 15c demonstrates the strong dependence of v_∞/v_{esc} on v_s^2/v_{esc}^2, which is properly (within 10%) described by Eq. (62) over two decades in v_s^2/v_{esc}^2. The variation of $\dot{M}$ along the evolutionary tracks of constant mass and luminosity (Fig. 15a) is caused purely by the finite cone angle effect, since $\dot{M}_{CAK}$ is constant as long as M, L, α, k are constant. We see that this effect is also well described by Eq. (64).

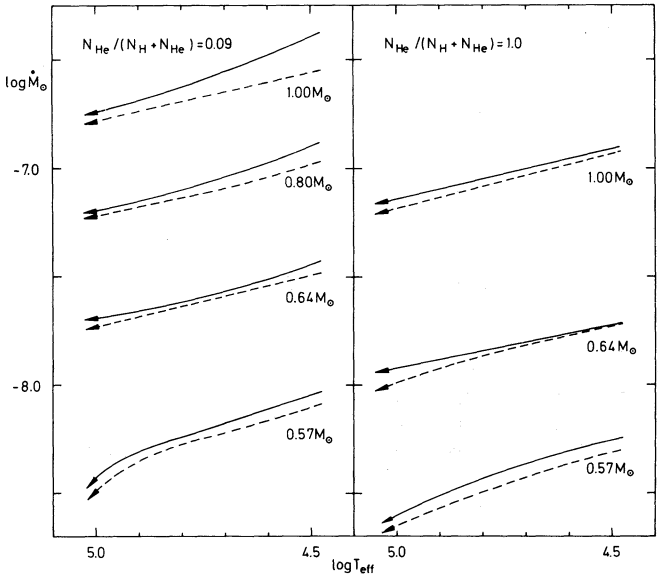

Fig. 15a. log $\dot{M}$ as function of log T_{eff} for wind models of CSPN along evolutionary tracks labelled by the stellar mass (fully drawn: numerical calculations; dashed: Eq. (63)). $k = 0.053$, $\alpha = 0.709$, $\delta = 0.051$ was chosen for all the models (see Pauldrach et al., 1988)

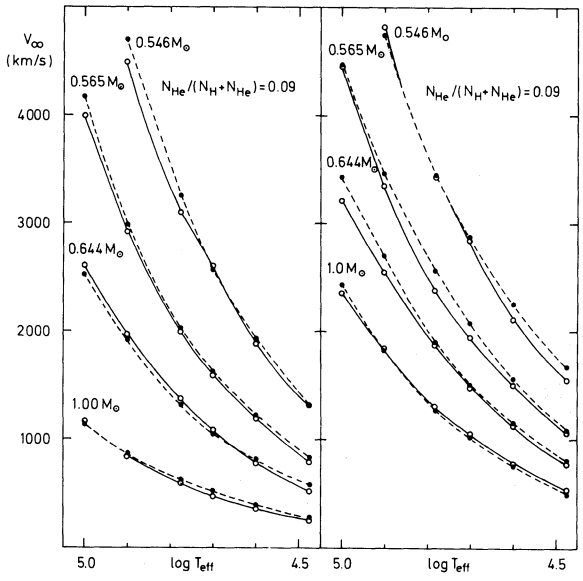

Fig. 15b. v_∞ as function of log T_{eff} for the same tracks as in Fig. 15a (fully drawn: numerical calculations; dashed: Eq. (62)). $\alpha = 0.709$, $\delta = 0.051$ was chosen for all the models

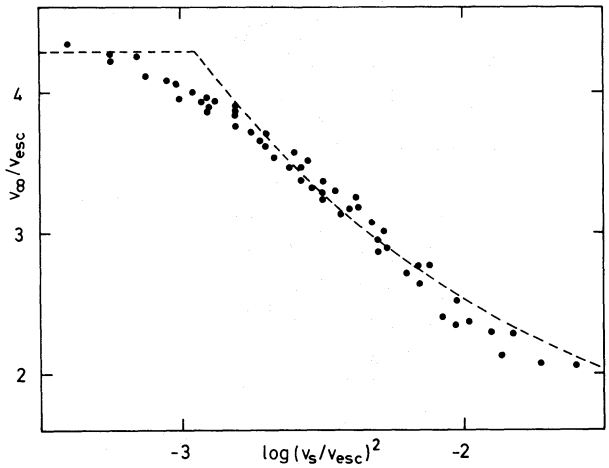

Fig. 15c. v_∞/v_{esc} as function of v_s^2/v_{esc}^2 for wind models of CSPN. The dots are the results of the numerical calculations, whereas the dashed line follows from Eq. (62). $\alpha = 0.709$, $\delta = 0.051$ was chosen for all the models

8. Conclusions and future work

In the preceding sections we were able to disentangle analytically the different effects working in radiation driven winds, when the radial streaming approximation is dropped and the finite cone angle of the photospheric disk is taken into account. It was shown that differential increase of the line force increases the acceleration of the wind when going outwards. The mass-loss rate, however, drops, because the absolute strength of the line force is smaller in the region around the critical point. Both effects are damped as soon as the geometrical extension of the photosphere – characterized by v_s^2/v_{esc}^2 – is increased. The ionization parameter δ in the line force has a similar influence.

The approximate analytical solution of the dynamical equations yielded formulae for v_∞/v_{esc} and $\dot{M}$ as functions of the stellar parameters L, M, R_* and the line force parameters k, α and δ. Thus, $\dot{M}$ and v_∞/v_{esc} can be easily computed provided that this line force parameter triple is given. However, at the moment, parameter sets of (k, α, δ) are available only for an approximate treatment of NLTE metal occupation numbers in the radiation driven winds (Abbott, 1982; PPK, Kudritzki et al., 1987). On the other hand, the recent work by Pauldrach (1987), Puls (1987) and Pauldrach et al. (1988a, b), which includes a detailed multi level NLTE treatment, has led to significant changes in (k, α, δ) for selected objects. Thus the next step for the future work is to investigate the general behaviour of k, α, δ as function of stellar

parameters including the detailed NLTE physics. This work is presently under way in our group.

Acknowledgements. It is a pleasure to thank our colleagues Henny Lamers and Martin Groenewegen (Utrecht) for critical comments on an earlier version of this paper. This work was supported by the Deutsche Forschungsgemeinschaft under grant Ku 474/11-3 and by the National Science Foundation through grant AST-8505919 and in part by the National Aeronautics and Space Administration through grant NAGW-766 to the University of Colorado.

Appendix 1

Here we briefly discuss the behaviour of the finite cone angle correction factor $CF(x, \alpha, \beta)$ as defined by Eqs. (13), (14), (15) and justify the approximations of Eqs. (48) and (50). Defining

$$\lambda(u, \beta) = u^2(1-h) = \frac{u}{\beta}((\beta+1)u-1) \tag{A1}$$

the correction factor $CF(x, \alpha, \beta)$ can be written as

$$CF = \frac{1}{\alpha+1}\frac{1}{\lambda}(1-(1-\lambda)^{\alpha+1}). \tag{A2}$$

The functions $\lambda(u, \beta)$ and $CF(\lambda, \alpha)$ are sketched in Fig. 16. We have $\lambda=1$ for $u=1$ and $\lambda=0$ for $u=(1+\beta)^{-1}$ and $u=0$. The minimum of λ is located at $u=(2(1+\beta))^{-1}$ and has the value of $\lambda_{\min} = -(4\beta(\beta+1))^{-1}$. $CF(\lambda, \alpha)$ is monotonically increasing with λ. We have $CF=(1+\alpha)^{-1}$ for $\lambda=1$ and $CF=1$ for $\lambda=0$. The value of CF at $\lambda=\lambda_{\min}$ can be approximated to first order by an expansion of CF in terms of small λ to be $CF_{\max}(\lambda_{\min}, \alpha, \beta) \approx 1+\alpha/(8\beta(\beta+1))$. The symmetric behaviour of $\lambda(u, \beta)$ on the interval $0 \le \lambda \le (2(1+\beta))^{-1} \le \lambda \le (1+\beta)^{-1}$ allows to approximate $CF^{1/1-\alpha}$ as

$$CF(u, \alpha, \beta)^{1/1-\alpha} \approx 1 + b_1 u - b_2 u^2, \quad 0 \le u \le (1+\beta)^{-1}. \tag{A3}$$

Demanding that $CF^{1/1-\alpha}=1$ for $u=(1+\beta)^{-1}$ and $CF^{1/1-\alpha}=1+(1/8)(\alpha/1-\alpha)(1/\beta(1+\beta))$ for $u=(2(1+\beta))^{-1}$ we obtain

$$b_1 = \frac{1}{2}\frac{\alpha}{1-\alpha}\frac{1}{\beta}$$

$$b_2 = b_1(\beta+1). \tag{A4}$$

For the interval $(1+\beta)^{-1} \le u \le 1$ the simplest, but sufficiently accurate approximation is

$$CF(u, \alpha, \beta)^{1/1-\alpha} \approx a_0 - a_1 u, \quad (1+\beta)^{-1} \le u \le 1. \tag{A5}$$

Because of $CF(1, \alpha, \beta)^{1/1-\alpha} = (1/1+\alpha)^{1/1-\alpha}$

$$a_0 = \left(1+\beta+\left(\frac{1}{1+\alpha}\right)^{1/1-\alpha}\right)\beta^{-1}$$

$$a_1 = +(1+\beta)\left(1-\left(\frac{1}{1+\alpha}\right)^{1/1-\alpha}\right)\beta^{-1}. \tag{A6}$$

Finally, we have to justify the approximation of Eq. (50) for the function

$$F(u, \alpha, \beta, \delta) = \left(\frac{2}{\alpha}\left(1-\left(\frac{1}{f_N(u, \alpha, \beta, \delta)}\right)^{1/1-\alpha}\right)\right)^{1/2}. \tag{A7}$$

Figure 17 shows for the example $\delta=0.05$ and $\beta=1.0$ that F increases rapidly with u to come close to the value F_0. The polynomical expansion given by Eq. (50) is therefore accurate enough to approximate F for the integral of Eq. (52).

Appendix 2

Here we justify the approximations of Eq. (55a), which yields the critical velocity v_c.

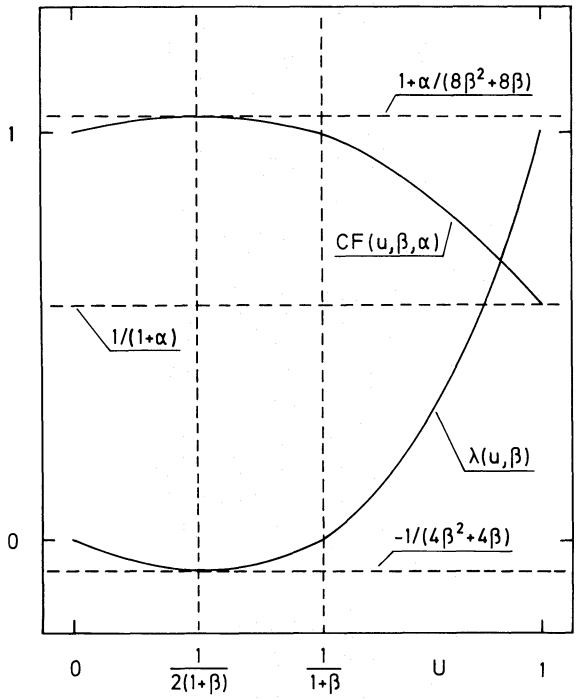

Fig. 16. Sketch of the functions $\lambda(u, \beta)$ and $CF(\lambda, \alpha)$

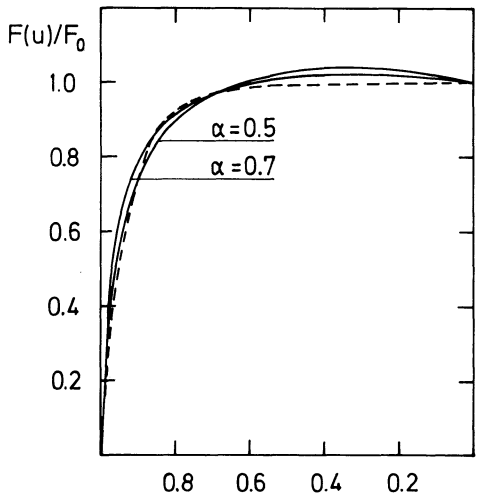

Fig. 17. The function $F(u, \alpha, \beta, \delta)$ (fully drawn) compared with the approximation of Eq. (50) (dashed) for the cases of $\alpha=0.5$ and 0.7. ($\delta=0.05$ and $\beta=1.0$ were chosen for this example)

The determination of v_c requires the knowledge of y at the sonic point and dy/dx at the critical point (see Eq. 55). For y_s a simple expression is obtained from the equation of motion (Eq. 5) by inserting the singularity condition (Eq. 21) and Eq. (53) and using the facts that $v=v_s$ and $f(x_c)\approx f(x_s)$

$$y_s/y_c=(1-\alpha)^{1/\alpha}, \tag{A8}$$

The far more complicate expression for $y'(x_c)$ follows from the total derivative of Eq. (5) and a subsequent application of L'Hospital's rule (see also PPK Eq. (A6)). After some calculation this leads to

$$y'_c=\frac{(9b^2 v_s^2/(16(1-\alpha)v_c^2+a/2)^{1/2}\, a^2 v_{esc}^4 v_s R_*}{(1-\alpha)^{5/2} x_c^2 v_c^3}-\frac{3b\alpha^2 v_{esc}^2 v_s^2 R_*}{4(1-\alpha)^3 v_c^4 x_c^2}$$

$$a=1+\frac{x_c v_c^2(1-\alpha)}{v_{esc}^2\alpha}+\frac{f''}{f}\frac{x_c^4 v_c^5(1-\alpha)^2}{2\alpha^3 v_s^2 v_{esc}^4}$$

$$b=1-\frac{f'}{f}\frac{2(1-\alpha)}{3\alpha}\frac{v_c^4 x_c^2}{v_s^2 v_{esc}^2}. \tag{A9}$$

Inserting Eq. (A8), (A9) in Eq. (55) and making use of Eq. (21) one gets

$$v_c=v_s\left(\frac{9b^2 v_s^2}{4(1-\alpha)^2 v_c^2}+\frac{2a}{(1-\alpha)}\right)^{1/2}\left(1+\left(1-\frac{3bd}{2a^2}\right)^{1/2}\right)\Big/ d$$

$$d=1-(1-\alpha)^{2/\alpha} \tag{A10}$$

Comparing the orders of magnitude of the terms in Eq. (A10) we find that this expression is fairly well approximated by Eq. (55a). (Note that $d=1$ was adopted to simplify the α-dependence. Since d varies only between 0.97 and 0.94 for $0.5\leq\alpha\leq 0.7$ this accurate enough.)

References

Abbott, D.C.: 1978, *Astrophys. J.* **225**, 893
Abbott, D.C.: 1980, *Astrophys. J.* **242**, 1183
Abbott, D.C.: 1982, *Astrophys. J.* **259**, 282
Castor, J., Abbott, D.C., Klein, R.: 1975, *Astrophys. J.* **195**, 157
Friend, D., Castor, J.: 1983, *Astrophys. J.* **272**, 259
Friend, D., Mac Gregor, 1984, *Astrophys. J.* **282**, 591
Friend, D., Abbott, D.C.: 1986, *Astrophys. J.* **311**, 701
Kudritzki, R.P., Pauldrach, A., Puls, J.: 1987, *Astron. Astrophys.* **173**, 293
Kudritzki, R.P., Méndez, R.H.: 1988, *Quantitative Spectroscopy and Model Atmospheres of Central Stars*, invited paper, Proc. of IAU Symp. No. **131**, *Planetary Nebulae*, ed. S. Torres-Peimbert, p. 273
Méndez, R.H., Kudritzki, R.P., Simon, K.P.: 1985, *Astron. Astrophys.* **142**, 289
Méndez, R.H., Kudritzki, R.P., Herrero, A., Husfeld, D., Groth, H.G.: 1988, *Astron. Astrophys.* **190**, 113
Panagia, N., Macchetto, F.: 1982, *Astron. Astrophys.* **106**, 266
Pauldrach, A., Puls, J., Kudritzki, R.P.: 1986, *Astron. Astrophys.* **164**, 86
Pauldrach, A.: 1987, *Astron. Astrophys.* **183**, 295
Pauldrach, A., Puls, J., Kudritzki, R.P., Méndez, R.H., Heap, S.R.: 1988, *Astron. Astrophys.* **207**, 123
Pauldrach, A., Kudritzki, R.P., Puls, J., Butler, K.: 1989, *Astron. Astrophys.* (in press)
Puls, J.: 1987, *Astron. Astrophys.* **184**, 227